MAGNETIC RESONANCE IN CHEMISTRY, VOL. 28, 355–363 (1990)

# A Novel Approach for Evaluating the NMR Spectra of Spinning Solids: Application to the Case of Chemical Exchange

**Lucio Frydman and Benjamin Frydman***
Catedra de Fitoquimica, Facultad de Farmacia y Bioquimica, Universidad de Buenos Aires, Junin 956, 1113 Buenos Aires, Argentina

**An approach is introduced that allows the evaluation of the effects of magic-angle spinning (MAS) in the NMR spectra of inhomogeneously broadened spin-$\frac{1}{2}$ nuclei. The method, which consists in replacing the time-dependent MAS Hamiltonian by a set of three time-independent Hamiltonians, is able to predict one of the main characteristics of the MAS experiment, namely the appearance of rotor echoes. Spectra were calculated using this approach and compared with $^{13}C$ NMR spectra of model compounds, showing good agreement in the range of spinning rates normally used. A simple extension of the method also makes it useful for simulating some cases of variable-angle spinning NMR. Although the approach is suitable for the evaluation of normal MAS NMR spectra, its main applications may be found in cases where the spin Hamiltonian is no longer self-commuting. As an example, the method was employed for analysing the case of an exchange process between two equally populated chemically equivalent sites. Calculated spectra obtained in this way allowed the correct reproduction of the changes observed in the MAS NMR spectra of two compounds which are known to undergo reorientations in the solid state. Further possible applications of the approach are discussed.**

KEY WORDS Solid-state NMR Magic angle spinning Solid-state dynamics

## INTRODUCTION

The considerable growth that the applications of NMR have experienced in the fields of physics, chemistry and biology can be ascribed to a large extent to the strong dependence which the resonance frequencies of the nuclei under observation show on the electronic environment at each site. However, this ability of NMR is usually hampered when the spectra are recorded in solids, owing to the considerable broadenings introduced in the resonances of the nuclei by the anisotropic character of the dipolar, chemical shift or quadrupolar interactions. It was first realized by Andrew *et al.*[1] and by Lowe[2] that if the anisotropic parts of the different interactions transform as second-rank tensors, high-speed spinning of the sample about an axis inclined at 54.74° with respect to $B_0$ (magic-angle spinning, MAS) will average the interactions to their isotropic values. This experiment has found its widest applications since Schaefer and Stejskal[3] showed its usefulness for recording the solid-state NMR spectra of dilute spin-$\frac{1}{2}$ nuclei such as $^{13}C$, $^{31}P$ or $^{15}N$. In these cases, MAS can be successfully employed for collapsing the chemical shielding powder patterns of the nuclei to their isotropic values, provided that the rates of sample rotation which are used are larger than the breadth of the tensor. In fact, this fast MAS experiment can be viewed as a particular case of the fast variable-angle spinning (VAS) experiment,[4–6] in which the spectrum arising from a sample which is rotated fast about an axis inclined at an angle $\beta$ with respect to $B_0$ shows the shielding powder patterns of the different nuclei scaled by a factor of $(3\cos^2\beta - 1)/2$.

One of the most widespread applications of solid-state NMR is the use of powder pattern line-shape analyses in order to evaluate the nature of dynamic processes which may occur in solids, such as chemical exchange or molecular motions.[7] As has been shown by Waugh and co-workers,[8,9] this clear information which is obtained from static samples may also be preserved in the MAS case, but only as shifts, broadenings or changes of intensities in the side-band spectrum. In order to take into account the effects of a dynamic process, it is necessary to add a dissipative term to the time-dependent MAS Hamiltonian, which precludes the analytical calculation of a time-evolution operator, and therefore different tactics have been adopted in order to retrieve the spectral information available from this experiment.

A simple approach has been used in cases where the dynamic process involved jumps of nuclei between sites with different isotropic chemical shifts, since then the analysis could be limited to an evaluation of the effects introduced by the exchange on the line shape of the centre-bands without taking into account the possible effects introduced by the spinning.[10,11] The first solution proposed for the quantitative evaluation of the case of nuclei exchanged between sites with equal isotropic chemical shifts was based on the average Hamiltonian

* Author to whom correspondence should be addressed.

0749–1581/90/040355–09 $05.00


*Received 22 November 1989*
*Accepted 27 December 1989*

theory,[9] and allowed the calculation of the line shapes of the spectral centre-bands of the nuclei for cases where the jump rates were smaller than the spinning speeds. 2D NMR and related techniques have also been used for analysing the nature of dynamic processes in rotating solids, since they allow the monitoring of the effects of the exchange on the side-bands intensities; their use has been restricted, however, to dynamic cases which take place in the slow exchange regime.[12,13] Finally, the problem has recently been solved in a general form by Schmidt and Vega[14] using the Floquet formalism. By use of this relatively complex mathematical treatment, the full side-band spectra of exchanging nuclei in solids could be calculated for arbitrary rates of exchange and spinning speeds. Moreover, this approach has already been found to be useful for the characterization of reorientational processes in organic solids.[15,16]

In this paper, a novel approach is presented for the evaluation of the spectra arising from rotating solids. As is shown in the following section, it is possible to simulate the centre-bands of solids rotating at different angles with respect to $B_0$ by periodically replacing the time-dependent Hamiltonian of each spin-packet by three time-independent Hamiltonians. Moreover, by introducing a small number of simple assumptions, the present approach is also able to produce FID signals which show the main property of the MAS experiment, namely, the formation of rotational echoes. In general, good agreement was found between spectra simulated using this approximation and spectra recorded under different experimental conditions. Although the present approach can be considered as a fast method for the recovery of the chemical shielding tensor parameters from MAS spectra, its usefulness can be best exemplified in cases where the spin Hamiltonian is no longer self-commuting at different times. In order to illustrate this property, the method was employed to evaluate the effects which are introduced in the spectra of spinning solids by the presence of molecular motions. For the case where the exchanging nuclei can jump between two sites, analytical expressions valid for any rate of exchange can be found for the evolution operator which is used in the spectral simulations. Predictions obtained in this way were compared with spectra recorded over a large range of temperatures and spinning rates for two compounds which are known to undergo molecular reorientations in the solid state; the general agreement that is found is good.

## RESULTS

### Chemical shift interaction in rotating solids

The events which take place in a rotating powder are usually described in a reference frame fixed on the rotor, which is spinning (in Hz) at a rate $\nu_R = \omega_R/2\pi$ about an axis which makes an angle $\beta$ with respect to the magnetic field. In this case, the rotating frame spin Hamiltonian of each crystallite can be written (in frequency units) as[17]

$$\begin{aligned}\mathscr{H}(\varphi, \theta, \psi; t) = &- \bar{\omega} I_z - \frac{\Delta\omega}{2}\left[\frac{1}{2}(3\cos^2\beta - 1)\right. \\ &\left.\times (3\cos^2\theta - 1 + \eta\sin^2\theta\cos 2\psi)\right] I_z \\ &- \Delta\omega[g_1\cos(\omega_R t + \phi_1) \\ &+ g_2\cos(2\omega_R t + \phi_2)] I_z \\ &= \omega_0 I_z + \omega(t) I_z \end{aligned} \quad (1)$$

where $\bar{\omega}$ is the isotropic frequency of the spins with respect to the transmitter, $\Delta\omega$ is the chemical shift anisotropy, $\eta$ is the asymmetry parameter of the tensor, and $g_k$, $\phi_k$ ($k = 1, 2$) are functions of $\eta$ and of the Euler angles $\varphi$, $\theta$ and $\psi$ which relate the principal axis system (PAS) of the shielding tensor in each crystallite to the rotor frame.

Since this Hamiltonian is time-dependent but self-commuting at all times, the evolution operator for each orientation can be evaluated as

$$U(\varphi, \theta, \psi; t) = \exp\left[-i\int_0^t \mathscr{H}(\varphi, \theta, \psi; t')\,dt'\right] \quad (2)$$

With $U(\varphi, \theta, \psi; t)$ it is possible to evaluate the signal $G(\varphi, \theta, \psi; t)$ which will observed for each crystallite after a 90° pulse or a cross-polarization sequence as the mean value of the $I_+$ operator at time $t$:

$$G(\varphi, \theta, \psi; t) = Tr[U(\varphi, \theta, \psi; t) I_x U^{-1}(\varphi, \theta, \psi; t) I_+] \quad (3)$$

Moreover, since $\mathscr{H}$ is linear in $I_z$, it is possible to describe $G(\varphi, \theta, \psi; t)$ as a vector whose real and imaginary components are given by an evolved phase $\phi(t)$:

$$\phi(t) = \omega_0 t + \int_0^t \omega(t')\,dt' \quad (4)$$

As has been shown,[8] these equations can be useful in order to understand some of the magic properties which are involved in the MAS averaging process. When $\beta = \beta_m = 54.74°$, $P_2(\cos\beta_m) = 0$ and the time-independent frequency of the spin packets becomes equal to the isotropic frequency. Nevertheless, the fact that the sample is spinning will introduce a change in the resonance frequency of each crystallite with time and, since for different initial orientations each spin-packet experiences a different resonance frequency, there will be a dephasing of the spin-packets which contributed to the initial macroscopic magnetization vector. It is a property of the MAS process, however, that after a complete revolution of the rotor, as the crystallites return to their initial orientations with respect to $B_0$, the phases which have been accumulated by each of the spin-packets become equal to the phase that would have been accumulated by a magnetization vector processing at the isotropic frequency of the interaction. At this time ($T_R$), the total magnetization has regained its original magnitude, giving rise to the formation of a rotor echo; the dephasing sequence then starts again.

Figure 1(A) illustrates the mechanical motion of the chemical shielding PAS of a single crystallite on MAS. Also shown is the well known fact that the magic axis of

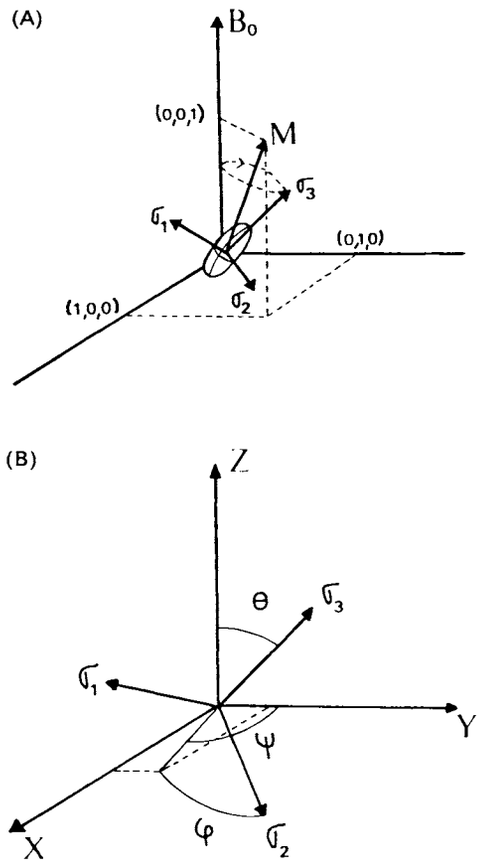


**Figure 1.** (A) Zeeman coordinate system showing the mechanical motion of the PAS of a crystallite upon spinning. (B) Definition of the Euler angles used, which relate the orientation of the PAS of a crystallite to the Zeeman axis system (ZAS).

rotation (M) has the direction of the diagonal of a cube in which the magnetic field lies along one of the edges. Therefore, it could be of interest to analyse which are the results that may be expected if the sample, instead of being continuously rotated about M, performs discrete jumps between the three orthogonal directions which define M. As will be exemplified below, this three-axis hopping approach, which is reminiscent of the technique used by Bax *et al.*[18] in order to obtain line narrowing in inhomogeneously broadened solids, predicts spectra which for most of the normal experimental conditions closely resemble the spectra which are obtained using the MAS technique.

From the discussion introduced with Eqns (1)–(4), it is clear that the case of spinning solids subjected to the chemical shift interaction can be treated in a classical way. Therefore, in order to develop the present model, each spin-packet will be considered as a magnetization vector which can evolve under the influence of three possible frequencies, one for each of the orientations that the crystallite can adopt with respect to $B_0$. In order to calculate these frequencies, it is convenient to define a fixed Zeeman axis system (ZAS) to which the PAS of each crystallite can be related through a set of $(\varphi, \theta, \psi)$ Euler angles; and then to evaluate the rotating-frame frequencies of each crystallite when $B_0$ points along the $X$, $Y$ and $Z$ axes of the ZAS (Fig. 1(B)). The chemical shielding tensor in the ZAS can be obtained by use of the rotation matrix $R(\varphi, \theta, \psi)$ as

$$\sigma^{ZAS} = R(\varphi, \theta, \psi)\sigma^{PAS}R^{-1}(\varphi, \theta, \psi) \tag{5}$$

where $\sigma^{PAS}$ is a diagonal matrix whose elements are the principal values $\sigma_1$, $\sigma_2$ and $\sigma_3$ of the chemical shielding tensor. The three frequencies which are needed can be found, after suitable truncation, as the projections of $\sigma^{ZAS}$ along the three possible orientations of $B_0$:

$$\begin{aligned}
\omega_{xx}^{ZAS} &= \omega_1 + \Delta\omega_1 \cos^2\psi \sin^2\theta \\
&\quad + \Delta\omega_2(\cos\psi\cos\theta\sin\varphi + \sin\psi\cos\varphi)^2 \\
\omega_{yy}^{ZAS} &= \omega_1 + \Delta\omega_1 \sin^2\psi \sin^2\theta \\
&\quad + \Delta\omega_2(\sin\psi\cos\theta\sin\varphi - \cos\psi\cos\varphi)^2 \\
\omega_{zz}^{ZAS} &= \omega_1 + \Delta\omega_1 \cos^2\theta + \Delta\omega_2 \sin^2\theta \sin^2\varphi
\end{aligned} \tag{6}$$

where $\omega_i = \gamma B_0 \sigma_i$ $(i = 1, 2, 3)$, $\Delta\omega_1 = \omega_3 - \omega_1$ and $\Delta\omega_2 = \omega_2 - \omega_1$.

Once the three evolution frequencies are known, it is necessary to propose a sequence of events which will allow the simulation of the effects of the spinning process. Since the projections of the magic axis M on the three axes of the ZAS are equal, and the averaging mechanism of MAS is of a coherent type, the simplest sequence which might be proposed in order to mimic the $n$th rotor period of a FID arising from a rotating sample is

$$\omega(t) = \begin{cases} \omega_{xx}^{ZAS} & (n-1)T_R \leqslant t < (n-1)T_R + T_R/3 \\ \omega_{yy}^{ZAS} & (n-1)T_R + T_R/3 \leqslant t < (n-1)T_R + 2T_R/3 \\ \omega_{zz}^{ZAS} & (n-1)T_R + 2T_R/3 \leqslant t < nT_R \end{cases} \tag{7}$$

or any other sequence in which $\omega_{xx}^{ZAS}$, $\omega_{yy}^{ZAS}$ and $\omega_{zz}^{ZAS}$ alternate in a similar way.

It is convenient to evaluate which is the phase that will be accumulated by each spin-packet after a full rotor period, since this is the phase that will determine the spectral line shapes in the 'fast-rotation' limit. From Eqn (7), this angle can be calculated as

$$\phi_{RP} = \left(\frac{\omega_{xx}^{ZAS} + \omega_{yy}^{ZAS} + \omega_{zz}^{ZAS}}{3}\right)T_R \tag{8}$$

which, by use of Eqn (6), can be shown to be

$$\begin{aligned}
\phi_{RP} &= \gamma B_0\left(\frac{\sigma_1 + \sigma_2 + \sigma_3}{3}\right)T_R \\
&= \bar{\omega}T_R
\end{aligned} \tag{9}$$

i.e. after a full rotor period all the spin-packets will have evolved the same phase, regardless of their initial orientation. Therefore, if $T_R$ is small ($\nu_R \gg \Delta\omega$), or if the FID is sampled at a rate $\nu_R$, Eqn (7) predicts for each chemically inequivalent nucleus a spectrum composed of a single sharp resonance at $\bar{\omega}$, as happens to be the case in the actual MAS experiment.

In order to analyse the potential uses of these predictions, the powder-averaged signals which can be obtained from Eqns (6)–(9) were compared with experimentally recorded spectra. Figure 2 shows the MAS spectra of the model compound hexamethylbenzene (HMB) recorded at different spinning speeds, together with the Fourier transforms of the time-domain signal

$G(t)$:

$$G(t) = \int_0^{2\pi}\int_0^{2\pi}\int_0^{\pi} \exp[i\phi(\varphi, \theta, \psi; t)] \sin\theta \, d\theta \, d\varphi \, d\psi \tag{10}$$

In order to obtain these simulations, the $^{13}C$ chemical shift parameters were taken from the single-crystal measurements[19] and only the rotor frequencies (i.e. the times $T_R$) were changed in each case. As can be seen, there is good agreement between the experimental results and the simulations. Although the magnetization path of each crystallite is dependent on the particular sequence assumed for the evolution frequency (i.e. $\omega_{xx} \rightarrow \omega_{yy} \rightarrow \omega_{zz}$, $\omega_{yy} \rightarrow \omega_{zz} \rightarrow \omega_{xx}$, etc.), simulations showed that the total powder spectrum was insensitive to this selection.

In summary, the approach presented above consists in replacing the spinning about the magic axis by jumps about the three orthogonal axes shown in Fig. 1(B), with the assumption that the sample remains one third of a rotor period along each orientation. This may suggest an extension of the present approach to the case of variable-angle spinning (VAS), where the sample is rotated about an axis inclined an angle $\beta$ with respect to $B_0$. This time the method would consist in replacing the effects of the spinning by periodic jumps of the sample about three orthogonal axes, with relative residence times in each of the axes proportional to $\sin^2\beta\cos^2 45$, $\sin^2\beta\sin^2 45$ and $\cos^2\beta$. Following the approach used for the simulation of the MAS case, the simplest sequence of frequencies which can be proposed for the $n$th rotor period of a sample undergoing VAS is

$$\omega(t) = \begin{cases} \omega_{xx}^{ZAS} & (n-1)T_R \leqslant t < (n-1)T_R + T_R \sin^2\beta/2 \\ \omega_{yy}^{ZAS} & (n-1)T_R + T_R \sin^2\beta/2 \leqslant t \\ & \quad < (n-1)T_R + T_R \sin^2\beta \\ \omega_{zz}^{ZAS} & (n-1)T_R + T_R \sin^2\beta \leqslant t < nT_R \end{cases} \tag{11}$$

The isotropic centre band that Eqn (11) predicts for a powdered sample in the fast spinning limit can be obtained by computing the phase which is evolved by each spin-packet during a full rotor period $T_R$:

$$\phi_{RP}(\varphi, \theta, \psi, \beta) = \left(\omega_{xx}^{ZAS}\frac{\sin^2\beta}{2} + \omega_{yy}^{ZAS} \times \frac{\sin^2\beta}{2} + \omega_{zz}^{ZAS}\cos^2\beta\right)T_R \tag{12}$$

By use of the expressions of $\omega_{xx}^{ZAS}$, $\omega_{yy}^{ZAS}$ and $\omega_{zz}^{ZAS}$ given in Eqn (6), the predicted isotropic phase can be shown to be

$$\phi_{RP}(\varphi, \theta, \psi, \beta) = \left\{\bar{\omega} + \frac{(3\cos^2\beta - 1)}{2}\frac{(\omega_3 - \bar{\omega})}{2} \times \left[3\cos^2\theta - 1 + \left(\frac{\omega_1 - \omega_2}{\omega_3 - \bar{\omega}}\right) \times \sin^2\theta\cos 2\varphi\right]\right\}T_R \tag{13}$$

which yields a spectrum for the whole sample which consists of a chemical shielding powder pattern scaled by a factor $(3\cos^2\beta - 1)/2$ and centred at $\bar{\omega}$. Indeed, this is the well known result predicted by Eqn (1) for a powder which spins fast about an axis inclined an angle $\beta$ with respect to $B_0$.[4]

In principle, an approach similar to that used for simulating powder spectra in the MAS case could be applied here, by changing the frequency of the spin-packets from $\omega_{xx}^{ZAS}$ to $\omega_{yy}^{ZAS}$ to $\omega_{zz}^{ZAS}$. However, it was found that in contrast to the MAS case, where the order of the $\omega_{ii}^{ZAS}$ did not influence the shape of the total powder spectra, the side-band pattern of the (VAS) spectral simulations were dependent on the order of the $\omega_{ii}^{ZAS}$. In most cases, better agreement with the experimental data was found when the first evolution frequency of each rotor period corresponded to the axis in which the residence time of the sample was longest. Figure 3 shows powder spectra calculated with this approach, together with experimental spectra of calcium formate recorded at different spinning angles. As with HMB, the chemical shielding parameters used were available from single-crystal work,[20] and the only experimental variables involved in the simulations were the spinning speed and the angle of rotation. It should be noted that since the sequences of the type described in Eqn (11) are not invariant with respect to 180° rotations, they predict spectra in which the separation between side-bands in the $\beta = 90°$ case is $\nu_R$ instead of

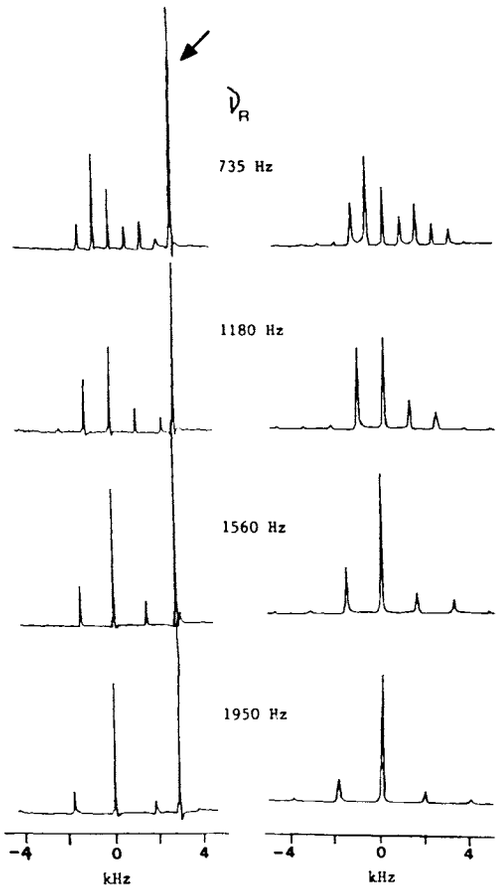


**Figure 2.** Left: experimental $^{13}C$ CPMAS NMR spectra of HMB at different spinning speeds. The signal marked with an arrow belongs to the methyl group. Right: spectra simulating the aromatic carbon signal. In all the spectra, the isotropic peak of the aromatic resonance was placed at the origin of frequencies.

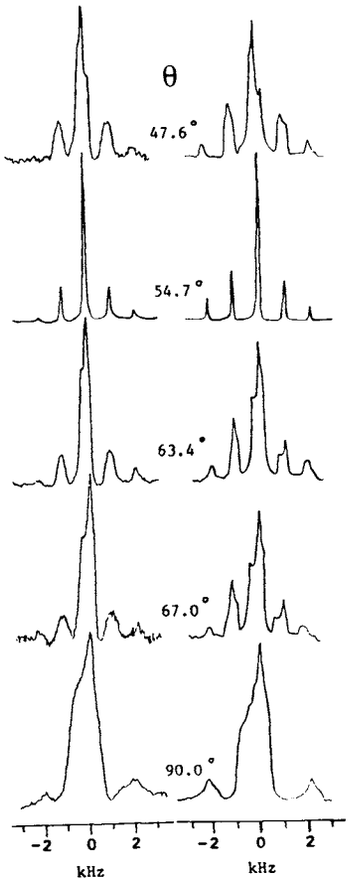


**Figure 3.** Left: experimental $^{13}C$ CPMAS NMR spectra of calcium formate spinning at 1100 Hz and at different angles with respect to $B_0$. Right: calculated spectra for each spinning angle, which was deduced from the line shape of the experimental centre-band. In the case of $\beta = 90°$, the simulation was performed assuming $\upsilon_R = 2200$ Hz (see text).

being $2\nu_R$. Therefore, the $\beta = 90°$ spectrum was simulated assuming a $T_R$ equal to $\frac{1}{2}\nu_R$. Moreover, this suggests that Eqn (11) is not useful for the simulation of spectra with $\beta$ close to 90° and that in such cases a more symmetric sequence should be employed.

## Effects of a two-site exchange process

As mentioned in the Introduction, one of the main applications of solid-state NMR is the characterization of motions in condensed phases. Although in the MAS case the static powders have collapsed to narrow centre-bands flanked by side-bands, the presence of exchange processes will still influence the spectra by precluding the refocusing of all the spin-packets of the sample at the end of each rotor period. Since an approach was introduced above which appeared to be useful for the evaluation of MAS spectra, it may be of interest to analyse whether the same approach can be employed for the simulation of MAS spectra of nuclei which are undergoing dynamic processes. In particular, when considering the case of an exchange process between two equally populated sites, a convenient starting point for its description is the classical equation for the transverse magnetization $M_I$ and $M_{II}$ of the sites:[21]

$$\begin{aligned} \frac{d}{dt} M_I &= i\omega_I M_I - kM_I + kM_{II} \\ \frac{d}{dt} M_{II} &= i\omega_{II} M_{II} + kM_I - kM_{II} \end{aligned} \tag{14}$$

where $\omega_I$ and $\omega_{II}$ are the frequencies of the sites, $k$ is the rate of exchange, and relaxation effects are not considered explicitly. Since in the treatment introduced in the preceding section the frequency of each nucleus was varied between three values which depend only on the orientation of the crystallite with respect to the ZAS, this approach will make available the MAS signal of the exchanging nuclei if Eqn (14) is replaced by three pairs of coupled differential equations with constant coefficients. To solve this, it is convenient to rewrite Eqn (14) in matrix form as

$$\frac{d}{dt} M = AM \tag{15}$$

Since $A$ is independent of time, $M$ at time $t + \Delta t$ can be calculated from $M$ at time $t$ as

$$M(t + \Delta t) = \exp(A\ \Delta t)M(t) \tag{16}$$

For the case of a two-site exchange process such as that under consideration, Eqn (16) can be rewritten as

$$\begin{aligned} M_I(t + \Delta t) &= e_1(\Delta t)M_I(t) + e_2(\Delta t)M_{II}(t) \\ M_{II}(t + \Delta t) &= e_3(\Delta t)M_I(t) + e_4(\Delta t)M_{II}(t) \end{aligned} \tag{17}$$

where $e_i(\Delta t)$ are the elements of $\exp(A\ \Delta t)$:

$$\begin{aligned} e_1(\Delta t) &= \frac{K}{1 + d^2} \{d^2[\exp(\Delta tr/2)] + \exp(-\Delta tr/2)\} \\ e_2(\Delta t) = e_3(\Delta t) &= \frac{Kd}{1 + d^2} [\exp(\Delta tr/2) - \exp(-\Delta tr/2)] \\ e_4(\Delta t) &= \frac{K}{1 + d^2} [\exp(\Delta tr/2) + d^2 \exp(-\Delta tr/2)] \end{aligned} \tag{18}$$

with

$$\begin{aligned} K &= \exp\left[ -k + i\left(\frac{\omega_I + \omega_{II}}{2}\right)\right] \Delta t \\ d &= \frac{r + i(\omega_I - \omega_{II})}{2k} \\ r &= [4k^2 - (\omega_I - \omega_{II})^2]^{1/2} \end{aligned} \tag{19}$$

As can be seen, $M$ depends parametrically on $k$ and also on $\Omega = (\omega_I + \omega_{II})/2$ and $\delta = \omega_I - \omega_{II}$.

In order to take into account the effects of the spinning, it is necessary to evaluate for each orientation $(\varphi, \theta, \psi)$ the projections $\Omega_{ii}$ and $\delta_{ii}$ $(i = x, y, z)$ of the tensors in the ZAS. Although this approach can be applied to any exchange case, the calculations will be developed for the case of flips of a molecule about a $C_2$ axis of symmetry. In these cases, a molecular reference system (MRS) can usually be found to which the PAS of the sites can be related through rotations $R$ and $R^{-1}$ about the $Z_{MRS}$ axis. The chemical shift tensor of each

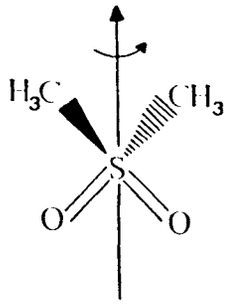


**Figure 4.** Proposed motion of the DMS molecules in the solid. A 180° flip about the main $C_2$ axis exchanges the orientations of the two methyls, and therefore the $PAS_I$ can be transformed into the $PAS_{II}$ by a 108° (2ε) rotation about $Z_{MRS}$.

site can be found in this system as

$$\omega_I^{MRS} = R(\varepsilon, 0, 0)\omega^{PAS}R^{-1}(\varepsilon, 0, 0)$$
$$\omega_{II}^{MRS} = R(-\varepsilon, 0, 0)\omega^{PAS}R^{-1}(-\varepsilon, 0, 0) \qquad (20)$$

Moreover, this MRS is also convenient for the evaluation of $\Omega^{MRS} = (\omega_I^{MRS} + \omega_{II}^{MRS})/2$ and $\delta^{MRS} = \omega_I^{MRS} - \omega_{II}^{MRS}$:

$$\Omega^{MRS} = \begin{pmatrix} \omega_1 \cos^2 \varepsilon + \omega_2 \sin^2 \varepsilon & 0 & 0 \\ 0 & \omega_1 \sin^2 \varepsilon + \omega_2 \cos^2 \varepsilon & 0 \\ 0 & 0 & \omega_3 \end{pmatrix}$$

$$\delta^{MRS} = \begin{pmatrix} 0 & 2(\omega_1 - \omega_2)\cos \varepsilon \sin \varepsilon & 0 \\ 0 & 0 & 0 \\ 0 & 0 & 0 \end{pmatrix} \qquad (21)$$

which can now be related to the ZAS by the use of the rotation matrix $R(\varphi, \theta, \psi)$ that relates the MRS to the ZAS. This procedure leads to the six relationships which are needed for the evaluation of Eqn (17):

$$\Omega_{xx} = Ar_{11}^2 + Br_{12}^2 + Cr_{13}^2$$
$$\Omega_{yy} = Ar_{21}^2 + Br_{22}^2 + Cr_{23}^2$$
$$\Omega_{zz} = Ar_{31}^2 + Br_{32}^2 + Cr_{33}^2 \qquad (22a)$$
$$\delta_{xx} = Dr_{11}r_{12}$$
$$\delta_{yy} = Dr_{21}r_{22}$$
$$\delta_{zz} = Dr_{31}r_{32}$$

where

$$A = \omega_1 \cos^2 \varepsilon + \omega_2 \sin^2 \varepsilon$$
$$B = \omega_2 \cos^2 \varepsilon + \omega_1 \sin^2 \varepsilon \qquad (22b)$$
$$C = \omega_3$$
$$D = 4(\omega_1 - \omega_2)\sin \varepsilon \cos \varepsilon$$

and $r_{ij}$ are the elements of the Euler matrix $R$. With these equations and the initial condition $M_I(0) = M_{II}(0) = \frac{1}{2}$, it is possible to calculate the total time domain signal of the two sites $G(t)$ as

$$G(t) = \int_0^{2\pi} \int_0^{\pi} \int_0^{2\pi} [M_I(\varphi, \theta, \psi; t) + M_{II}(\varphi, \theta, \psi; t)]\sin \theta \, d\varphi \, d\theta \, d\psi \qquad (23)$$

The results obtained by Fourier transformation of this signal were compared with the variable-temperature spectra of dimethyl sulphone (DMS, Fig. 4), a compound which has been shown to perform 180° flips about its main $C_2$ molecular axis[22] and which will be used to check the predictions of the present theoretical model. Since the dynamics of solid DMS have already been measured in a $^{13}C$ NMR powder lineshape analysis,[22] from which the principal values of the chemical shift tensor and the jump angle 2ε also became available, no attempt to fit the experimental data was necessary. In all the simulations the chemical shift values were taken as $\omega_1 = \omega_3 = -940.8$ Hz, $\omega_2 = 470.4$ Hz ($\bar{\omega} = 0$, $\eta = 0$ and $\Delta\omega = 56$ ppm at 25.2 MHz $^{13}C$ frequency), and an angle of 108° was assumed between the $Y$ axes of $PAS_I$ and $PAS_{II}$. The rate constant $k$ was

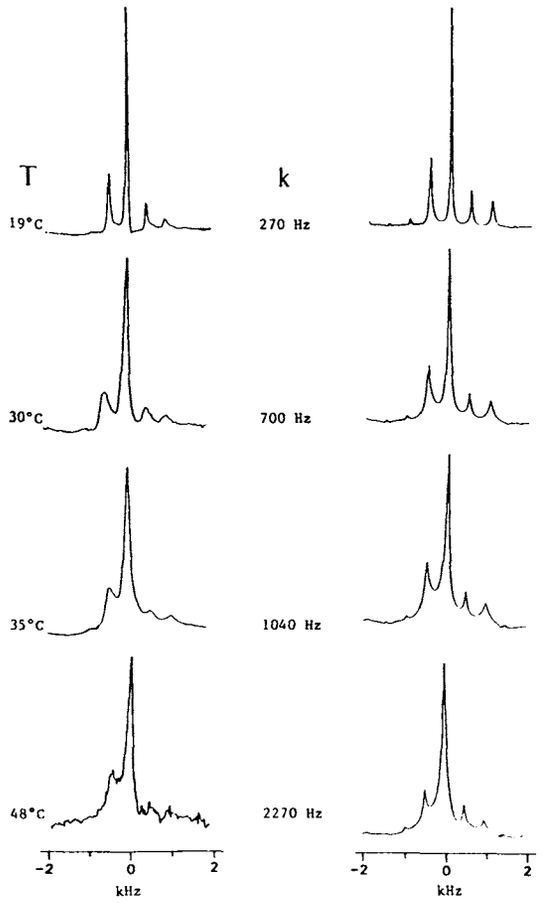


**Figure 5.** Left: experimental $^{13}C$ CPMAS NMR spectra of DMS recorded at different temperatures and at a rotation rate of *ca.* 500 Hz. Right: spectra calculated for each temperature using the Arrhenius equation that can be deduced from Ref. 22. In the simulated spectra, a non-exchanging line width of 40 Hz was assumed. The blurring observed in the side-bands of some recorded spectra may be ascribed to small (*ca.* 20 Hz) variations in the spinning speed during long accumulations.

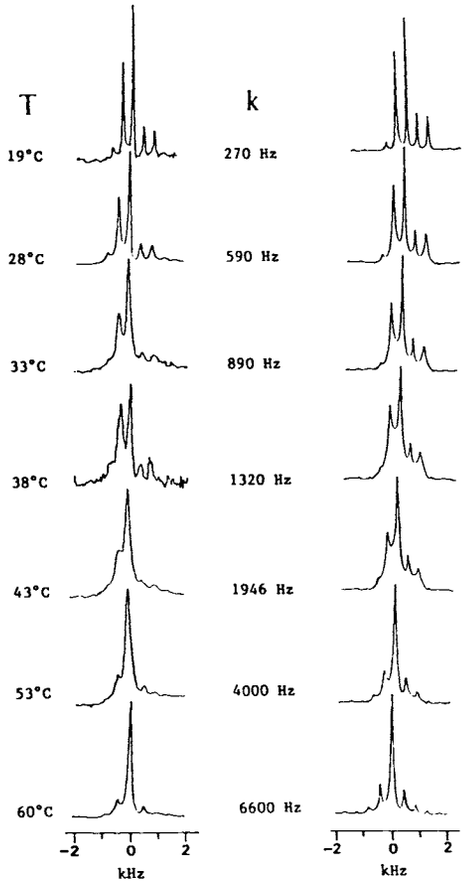


**Figure 6.** Left: experimental $^{13}C$ CPMAS NMR spectra of DMS recorded at different temperatures and at a rotation rate of *ca.* 400 Hz. Right: spectral simulation for each temperature. Other details as in Fig. 5.

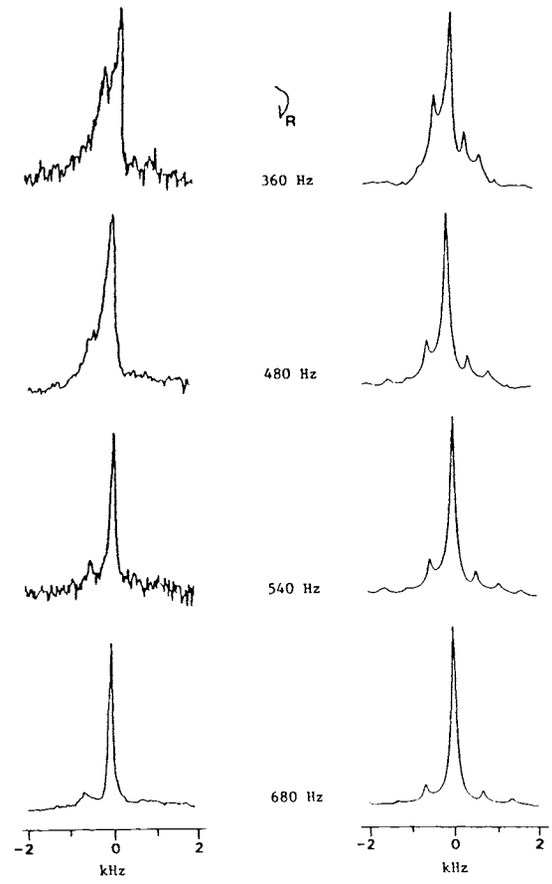


**Figure 7.** Left: experimental $^{13}C$ CPMAS NMR spectra of DMS recorded at 45 °C and at different spinning rates. Right: spectra simulated for each spinning speed. A flipping rate $k = 2260$ Hz was assumed in all cases. A non-exchanging line width of 50 Hz was used in the simulations.

also taken from the static powder analysis as $k = 5.44 \times 10^{13} \exp(-7601/T)$ Hz. Figures 5 and 6 show the spectra of DMS recorded at constant speed as a function of temperature, together with the simulations which correspond to each temperature. The centre-band and side-bands broaden as the temperature is increased from 20 to 45 °C, then they start to narrow again but displaying a pattern of side-band intensities which differs from that shown at lower temperatures. A similar behaviour is followed by the simulations, which exhibit only minor deviations from the experimental line shapes in the side-band intensities. The predictions of the present approach were also tested against spectra recorded at the temperature of maximum broadening (45 °C) using different spinning rates. These results are shown in Fig. 7, in which the decrease in the overlapping of the centre-band and the side-bands as the spinning speed is increased is evident both in the experimental data and in the simulations. In addition, a slight narrowing is noticeable in the line width of the centre-band as the rate of rotation becomes higher.

Although with the use of the 'calibration' sample DMS it was shown that the theoretical approach described previously is useful for evaluating the effects of chemical exchange from both qualitative and quantitative points of view, the application of the method to a more 'real' problem, as is the analysis of 180° ring flips in *para*-substituted aromatic compounds about their $C_2$ axes, will be briefly described. As has been shown recently,[16] the aromatic rings in γ-sulphanilamide perform the type of motion shown in Fig. 8, as a result of which the positions of C-2 and C-3 are exchanged with those of C-6 and C-5. For the purpose of simplicity, it will be assumed that the difference in the principal values of the chemical shifts of the exchanging nuclei is small enough to be taken into account as a residual line broadening. Although in order to perform the simulations it can be assumed that the jump angle

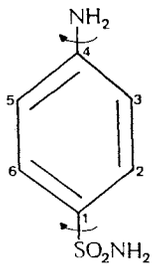


**Figure 8.** Structure of sulphanilamide (*p*-aminobenzenesulphonamide) showing the atom numbering and the axis of 180° rotations. $PAS_I$ can be transformed into $PAS_{II}$ by performing a 120° rotation about the $Z_{MRS}$ axis.

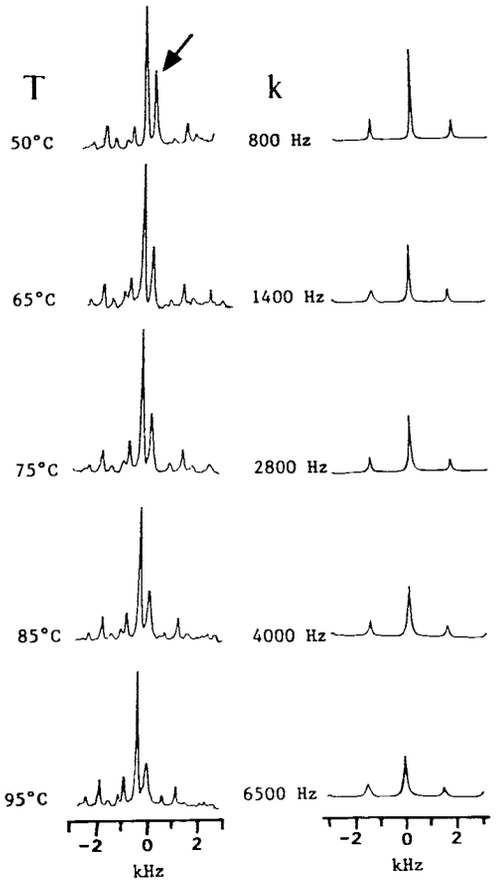


**Figure 9.** Left: experimental $^{13}C$ CPMAS NMR spectra of sulphanilamide at different temperatures. Right: simulations of the C-3 and C-5 resonance (labelled with an arrow) for different rates of phenyl flipping. In the simulations the isotropic frequency of the resonance was centred at zero, and a non-exchanging line width of 40 Hz was assumed. In contrast to the simulations of DMS, the same scaling factor was used for all the calculated spectra.

$2\varepsilon$ is 120°, it is also necessary to have available the values of $\omega_1$, $\omega_2$ and $\omega_3$. Since to our knowledge neither powder nor single-crystal $^{13}C$ NMR studies of this compound have been carried out, approximate values for these numbers were obtained by iterative fitting of the centre- and side-band intensities in the room-temperature spectrum ($\omega_1 = 5292$ Hz, $\omega_2 = 3276$ Hz and $\omega_3 = 1008$ Hz at 25.2 MHz $^{13}C$ NMR frequency). A further complication arose from the fact that the C-2–C-6 signal overlapped with the C-1 resonance. For this reason, simulations focused on the signal arising from the C-3–C-5 pair of nuclei.

The left-hand side of Fig. 9 shows the $^{13}C$ CPMAS NMR spectra of $\gamma$-sulphanilamide recorded at different temperatures. As can be seen, the spectra are affected by the molecular motion, a fact which is not only noticeable by the broadening introduced in the signals, but also by the sharp decrease in the signal intensities. The right-hand side of Fig. 9 shows spectra simulated using the approach described in Eqns (17)–(19). In order to assign each simulation to its temperature, a pool of spectra were computed using different rate constants $k$, and for each temperature the best fit was chosen. The simulations reproduce correctly the experimental spectra, making available the Arrhenius equation of the process $k = 2.8 \times 10^{10} \exp(-5630/T)$.

## EXPERIMENTAL AND COMPUTER CALCULATIONS

$^{13}C$ CPMAS NMR spectra were recorded at 25.2 MHz on a Varian XL-100-15 NMR spectrometer modified for performing the $^{1}H$ CP sequence with spin-temperature alternation. The probe is a laboratory-built single-coil system equipped with an external deuterium lock for field stabilization and a Macor-machined stator for sample spinning. In order to record the spectra, the samples were placed in boron nitride barrel-type rotors which were driven by air and showed long-term spinning stability (variations smaller than 20 Hz in the spinning rates during overnight accumulations). In the case of DMS, where spectra were recorded at slow spinning rates, rotation stability was achieved using rotors which were machined without driving flutes. The spinning rate was monitored using a system based on a device which detects reflected light from the half-painted rotor cap. In the variable-temperature operation, the spinning air was heated by means of a resistance heater driven by a temperature controller which monitored a thermocouple at the base of the stator assembly; the temperatures obtained in this way are considered accurate to $\pm 2$ °C.

All the spectra were recorded using a 2-ms contact time with fields matched at 62 kHz, and a 3-s repetition time. HMB was purchased from Aldrich and used without further purification. The 90% $^{13}C$-enriched calcium formate was prepared from enriched formic acid (MSD Isotopes) and calcium chloride. DMS was obtained by oxidation of dimethyl sulphide, and *ca.* 6000 transients were accumulated before obtaining each DMS spectrum. $\gamma$-Sulphanilamide was obtained by recrystallization of the drug from isoamyl alcohol, and an average of 20 000 transients were acquired for obtaining each spectrum of this compound.

One of the main advantages of the present approach is its relative simplicity, which is translated into an important saving of computational effort. This can be illustrated with the procedure followed in order to obtain the simulations of the non-exchanging MAS spectra. After a minimum bandwidth to be used in the simulations is specified, a sampling interval $\Delta t$ is calculated which not only gives the desired band width but which also fulfills the condition that the number of sampling times per rotor period ($T_R/\Delta t$) is an integral multiple of 3. Then, for each orientation $\varphi$, $\theta$, $\psi$ the three time propagators

$$X = \exp(i\omega_{xx}^{ZAS}\,\Delta t)$$

$$Y = \exp(i\omega_{yy}^{ZAS}\,\Delta t)$$

$$Z = \exp(i\omega_{zz}^{ZAS}\,\Delta t)$$

are evaluated. Starting from the initial condition $G(0) = \sin\theta$, it is possible to obtain the signal $G$ at time $n\,\Delta t$ from $G[(n-1)\,\Delta t]$ by multiplication with $X$, $Y$ or $Z$. The FID obtained in this way is added to the FID obtained for the other $\varphi$, $\theta$, $\psi$ Euler angles in order to

obtain the complete powder signal. In those cases where the isotropic frequency $\bar{\omega}$ has been placed at an integral multiple of $2\pi\nu_R$ or at zero, the MAS experiment is completely cyclic with period $T_R$, and it is sufficient to calculate the FID for times $0 \leqslant t \leqslant T_R$, and then to repeat this number until the total number of points achieves the desired digital resolution. Finally, since the equations that were developed did not take into account relaxation effects, these had to be introduced by multiplying the total time-domain signal by $\exp(-t/T_2)$ before Fourier transformation. This was the procedure used for obtaining the simulations shown in Fig. 2, for which the intervals $0° \leqslant \varphi, \theta, \psi \leqslant 180°$ were partitioned in 9° steps, giving a total of 8000 orientations; smaller angular increments did not introduce significant changes in the spectral shapes. Each of these powder calculations required about 50 s of CPU time in our microVAX 2000 computer.

A similar approach was used in the simulations of the dynamic MAS spectra, although in this case the presence of an energy-dissipative term in the Hamiltonian makes necessary the evaluation of the $2^n$ points which comprise the FID. For each orientation $\varphi$, $\theta$, $\psi$, the FID of the spin-packet can be evaluated using the three groups of $e_i(\Delta t)$ ($i = 1, 2, 4$) of Eqn (17) which are evaluated for each of the pairs of $\Omega_{ii}$ and $\delta_{ii}$ ($i = x, y, z$) given in Eqn (22). In the spectra simulated for DMS and sulphanilamide, $18^3 = 5832$ powder orientations were used. Each spectrum, consisting of $2^9$ points, required about 4 min of CPU time in a microVAX 2000.

## DISCUSSION AND CONCLUSIONS

The method introduced for the simulation of MAS spectra can be said, in a sense, to be based on the geometrical properties of the spinning axis. Comparing the calculations with experimental spectra (not all of which are shown here), it can be concluded that the approach yields quantitatively acceptable chemical shift parameters in the range $\Delta\omega/2\pi\nu_R < 6$, which in $^{13}C$ and $^{15}N$ NMR is a range usually used for samples other than model compounds. Nevertheless, it is probable that the potential of the method does not lie in the simulation of normal MAS spectra, but rather in the evaluation of those cases where an additional term renders the spin Hamiltonian no longer self-commuting at different times, since then the evolution operator is not available by simple integration of the equations of motion. Although the linearity in the spin operators of the Hamiltonians which have been analysed here have allowed the use of magnetization vectors, the present approach can also be used if the density matrix formalism has to be employed.

There are some simple extensions to the exchange analyses described. Following the treatment introduced in Eqns (20)–(22), it is relatively straightforward to obtain the $\Omega_{ii}$ and $\delta_{ii}$ which are necessary to analyse the case where the chemical shift tensors of the two sites differ, or the case where the two sites are related by an arbitrary set of Euler angles. For two-site exchange processes, it is also relatively simple to analyse the case of unequally populated sites, for which an analytical recalculation of the $\exp(A\,\Delta t)$ matrix is necessary. Other effects that can be analysed with the equations described above are those introduced by a chemical exchange process on a sample which is spun at an angle other than 54.74°, an experiment which may be useful if resolution and sensitivity can be sacrificed for the sake of obtaining more complete line-shape information. Finally, it is also possible to extend the present approach to calculate the effects of a three-or-more site exchange process, although this case would require a numerical diagonalization of the exchange matrix $A$ for each orientation.

### Acknowledgement

This research was supported by the National Institutes of Health under Grant GM 11973 and by the Consejo Nacional de Investigaciones Cientificas y Tecnicas (CONICET). L.F. is grateful to CONICET for a fellowship. Enlightening discussions with Professor Shimon Vega (Weizmann Institute) are also gratefully acknowledged.

## REFERENCES

1. E. R. Andrew, A. Bradbury and R. G. Eades, *Nature (London)* **182**, 1659 (1958); E. R. Andrew, *Philos. Trans. R. Soc. London, Ser. A* **299**, 505 (1981).
2. I. J. Lowe, *Phys. Rev. Lett.* **2**, 285 (1959).
3. J. Schaefer and E. O. Stejskal, *J. Am. Chem. Soc.* **98**, 1031 (1976).
4. E. O. Stejskal, J. Schaefer and R. A. MacKay, *J. Magn. Reson.* **25**, 569 (1977).
5. E. M. Menger, D. P. Raleigh and R. G. Griffin, *J. Magn. Reson.* **63**, 579 (1985).
6. N. K. Sethi, D. M. Grant and R. J. Pugmire, *J. Magn. Reson.* **71**, 476 (1987).
7. H. W. Spiess, *Molecular Rotation and Nuclear Spin Relaxation*. Springer, Berlin (1978).
8. M. Matti Maricq and J. S. Waugh, *J. Chem. Phys.* **70**, 3300 (1979).
9. D. Suwelack, W. P. Rothwell and J. S. Waugh, *J. Chem. Phys.* **73**, 2559 (1980).
10. B. H. Meier and W. L. Earl, *J. Am. Chem. Soc.* **107**, 5553 (1985).
11. L. Frydman, A. C. Olivieri, L. E. Diaz, A. Valasinas and B. Frydman, *J. Am. Chem. Soc.* **110**, 5651 (1988).
12. A. P. M. Kentgens, E. de Boer and W. S. Veeman, *J. Chem. Phys.* **87**, 6859 (1987).
13. Y. Yang, M. Schuster, B. Blumich and H. W. Spiess, *Chem. Phys. Lett.* **139**, 239 (1987); Y. Yang, A. Hagemeyer, B. Blumich and H. W. Spiess, *Chem. Phys. Lett.* **150**, 1 (1988).
14. A. Schmidt and S. Vega, *J. Chem. Phys.* **87**, 6895 (1987).
15. A. Schmidt, S. O. Smith, D. P. Raleigh, J. E. Roberts, R. G. Griffin and S. Vega, *J. Chem. Phys.* **85**, 4248 (1986).
16. L. Frydman, A. C. Olivieri, L. E. Diaz, B. Frydman, A. Schmidt and S. Vega, *Mol. Phys.*, in the press.
17. E. T. Olejniczak, S. Vega and R. G. Griffin, *J. Chem. Phys.* **81**, 4804 (1984).
18. A. Bax, M. Szeverenyi and G. E. Maciel, *J. Magn. Reson.* **52**, 147 (1983).
19. S. Pausak, J. Tegenfeldt and J. S. Waugh, *J. Chem. Phys.* **61**, 1338 (1974).
20. J. L. Ackerman, J. Tegenfeld and J. S. Waugh, *J. Am. Chem. Soc.* **96**, 6843 (1974).
21. A. Abragam, *The Principles of Nuclear Magnetism*. Oxford University Press, London (1961).
22. M. S. Solum, K. W. Zilm, J. Michl and D. M. Grant, *J. Phys. Chem.* **87**, 2940 (1983).